RUPTURE DETECTION IN FATIGUE CRACK PROPAGATION

ROMAIN AZAÏS, ANNE GÉGOUT-PETIT, AND FLORINE GRECIET

This chapter is dedicated to piecewise-deterministic models for Fatigue Crack Propagation (FCP) with a particular focus on the estimation issues. In this setting, the process is usually observed on a temporal discrete grid and through an additive noise, which makes unknown both the continuous trajectory and the mode. A significative part of the chapter relies on the article [4].

1. Phenomenon of Crack Propagation

FCP in materials is a complex deterioration process which, under the action of cyclic stresses over an extended time period, modifies local properties of the materials. It begins by the apparition of micro-cracks which can propagate rapidly until the failure of the structure.

FCP is responsible for 50 to 90 percent [36] of all mechanical failures in metallic structure. Engineers have to take into account this phenomenom in the design and in life prediction of fatigue-critical structures such as aircrafts, offshore platforms, bridges, etc.

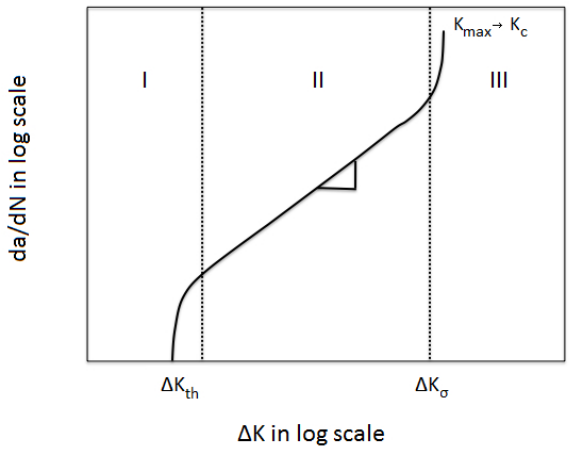

Figure 1.1. Schematic illustration of the different regimes of FCP. The vertical dashed lines indicate the transition between crack propagation regimes.

Data obtained from experimental tests provide the main source of information regarding fatigue of materials. If we denote a_t the length of the crack at time t, for

ductile materials, fatigue crack growth rate da_t/dt can be correlated with the cyclic variation of stress intensity factor ΔK_t. The typical logarithmic plot of da_t/dt versus ΔK_t is shown in Figure 1.1. The curve involves three regimes. In regime I, referred to as the crack initiation region, crack propagation is a discontinuous process which is extremely slow at very low values of ΔK_t. In regime II, a power-law relationship between crack growth rate and stress intensity factor range is observed. Finally, regime III corresponds to a quick and unstable crack growth leading to rupture when the stress intensity factor tends to the critical value K_c.

1.1. **Virkler's Data.** Experimental data obtained by Virkler et al. [39] is a well known source of information about fatigue of engineering materials. These data, available in the literature, are probably the most famous and frequently used data sets to model crack propagation. Many figures and studies presented in this chapter rely on analyses about these data. We describe the process of their acquisition in the next paragraph.

A total of 68 center-crack specimens of 2024-T3 aluminium alloys were tested under constant amplitude loading $\Delta\sigma = 48.28$ MPa at a stress ratio $R = 0.2$. During these tests, engineers used the same material containing initially identical artificial made 9 mm crack length where the crack initiation can be considered completed. The sample paths represent the evolution in time of the crack size for the 68 specimens, whose measures were performed until they reach the critical value K_c=49.8 mm. Measurements were taken every 0.2 mm in the range $9.0 \leq a_t \leq 36.2$ mm, every 0.4 mm in the range $36.2 \leq a_t \leq 44.2$ mm, and every 0.8 mm in the range $44.2 \leq a_t \leq 49.8$ mm.

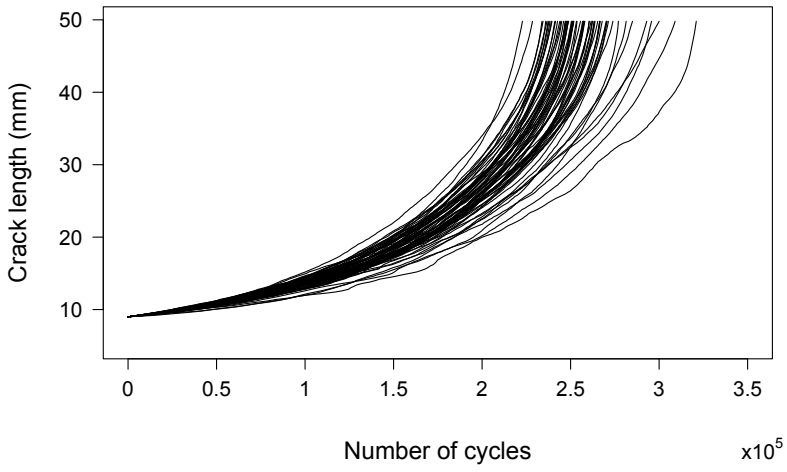

FIGURE 1.2. The 68 experimental crack length curves versus the number of cycles provided by [39].

A total of 164 measurements were taken for each of the 68 replicate specimens presented in Figure 1.2. These empirical data were used to build the FCP models of this chapter.

2. Modeling Crack Propagation

2.1. **Deterministic Models.** Generally, phenomenological laws used by mechanical engineers to model FCP are of the following form [25],

$$\frac{da_t}{dt} = L(t, \Delta K_t, K_{\max,t}, K_c, \sigma_{\max}, a_t, R), \tag{2.1}$$

with L a non-negative function and the different notations given in Table 2.1.

t	number of cycles
a_t	crack size
da/dt	fatigue crack growth rate
ΔK_t	range of the stress intensity factor
$K_{\max,t}$	maximum stress intensity factor, depending on t
K_c	fracture toughness
$\sigma_{\max}$	maximum stress amplitude in the loading spectrum
R	stress ratio defined by $R = K_{\min,t}/K_{\max,t}$
$\Delta\sigma$	stress range defined by $\Delta\sigma = \sigma_{\min} - \sigma_{\max}$

Table 2.1. Notations

Paris and Erdogan in [31] were the first to propose an equation of such a form. This equation, called Paris' law, only describes the linear part of the logarithmic relationship between FCP rate and stress intensity range (regime II). It is certainly the most used model because of its simplicity. It relates the change rate of crack size a_t with number of load cycles t through ΔK_t by the following equation,

$$\frac{da_t}{dt} = C(\Delta K_t)^m, \tag{2.2}$$

where C and m are constant parameters depending on the material. In most cases, ΔK_t is given by the relation

$$\Delta K_t = Y(a_t)\Delta\sigma\sqrt{\pi a_t},$$

where $Y(a_t)$ is a dimensionless factor that considers the crack shape and the geometry of the specimen, and $\Delta\sigma$ is the stress range.

Even with its popularity and its accuracy in describing the regime II of propagation, the model given by (2.2) is not well adapted to express the transition at the beginning of region III and it does not account for stress ratio effects. Many alternatives for FCP relations have been proposed to overcome the limitations of Paris' law. The Walker equation, introduced by Walker in [40], provided one of the first simple equations that accounted for the stress ratio R and is given by

$$\frac{da_t}{dt} = C[(1-R)^m K_{\max}]^p, \tag{2.3}$$

where C, m and p are the parameters of this law.

Forman, in [17], suggested a model called Forman's law. This law captures the rapid increase of growth in region III and includes the stress ratio R and the fracture toughness K_c. To do that, Paris' law equation was divided by a factor that would

reach zero when the stress intensity factor reaches a critical level. The general form of the Forman equation is

$$\frac{da_t}{dt} = \frac{C(\Delta K_t)^m}{(1-R)K_c - \Delta K_t}, \tag{2.4}$$

where K_c, the fracture toughness represents the value of the stress intensity factor required to reach failure. This equation can be rearranged to yield the following equality,

$$\frac{da_t}{dt} = \frac{C(1-R)^{m-1}K_{\max,t}^m}{K_c - K_{\max,t}}, \tag{2.5}$$

which shows that the equation has the capability to describe multiple stress ratio data sets.

Other authors such as Forman and Mettu in [18] proposed more complex models which account for the stress ratio R and describes the entire crack growth life taking into account both of the threshold of stress intensity range delimiting the regimes ΔK_{th}, ΔK_σ (see Figure 1.1) and therefore of the material fracture toughness K_c.

Nevertheless, Paris' law is still in wide use to model fatigue crack growth because it works well to describe the regime II of propagation with a low number of parameters.

2.2. **Sources of Uncertainties.** Based on engineering and macroscopic viewpoints, mechanical properties of material are often considered homogeneous. However, as shown on the Virkler's data presented in Figure 1.2, crack length data exhibit statistical variability which increases with the number of cycles. Other authors such as Ghonem and Dore in [19] or Wu and Ni in [43] show similar results.

The randomness observed is not an artifact of the measurement device but is due to the material behavior, even when data were obtained under the same loading condition in a strictly controlled environment with specimens cut from the same sheet. These random effects seem to vary not only from specimen to specimen but also during crack growth.

We can suppose that basic scientific knowledge of fatigue is not yet certain enough to describe in a strictly deterministic manner the propagation of cracks. It is not possible to propose a deterministic law which would be valid for any individual of an experiment even if the experiment is repeated under absolutely identical conditions.

This scatter is also shown on the logarithmic representation of the Virkler's results of crack growth rate in terms of stress intensity range ΔK_t represented in Figure 2.3. As schematized in Figure 1.1, a linear increase of da_t/dt is observed on the largest part of the propagation with some changes at the end and to a lesser extend, at the beginning.

Due to the amount of scatter, investigators have started using statistical models to characterize FCP behavior. It has been pointed out that the remaining scatter is due to the essentially random nature of fatigue crack growth which is a result of the relative inhomogeneity of the material. Deterministic models can not adequately describe crack growth behavior, and the variability in the data should be appropriately taken into account in the design and in analysis of fatigue-critical structure.

2.3. **Stochastic Models.** To take into consideration scatter observed on data, many authors were interested in stochastic models to describe the evolution of crack propagation in fatigue.

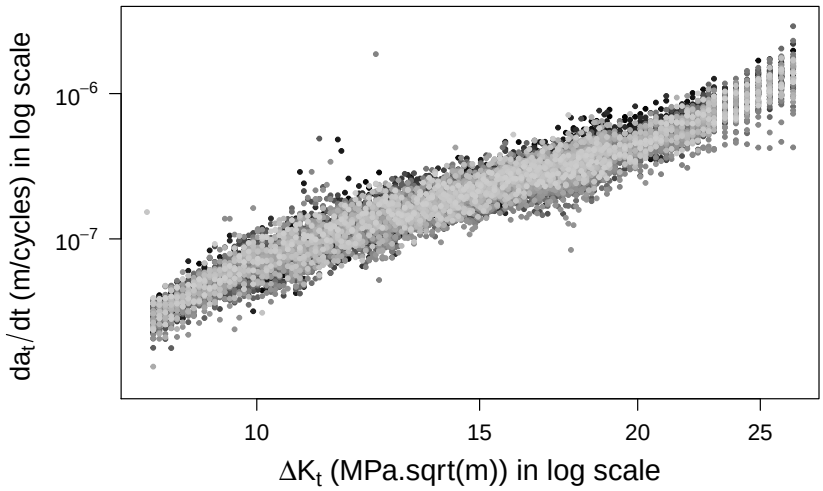

FIGURE 2.3. Crack growth rate in terms of ΔK_t computed from the 68 experiments provided in [39].

Some of them have proposed models to describe the process of crack initiation, see for instance [35, 24]. In [35], the authors proposed some empirical equations. They indicate a possible way towards a more detailed characterization of random microstructural effects of mechanical and fatigue properties of materials. The results can be used for the design of device.

One advantage of the stochastic model proposed by [24] is that it is applied to two different data sets of Ohtani et al. in [28, 29] for which experimental data of crack initiation are available. This model uses concepts of damage accumulation and critical damage required for failure, to predict the crack initiation distribution and their early growth. Note that the number of data based on crack initiation is very low and this part of propagation is difficult to model. It is not the case for the propagation and fracture regimes of the crack we are interested in and for which there are a lot of models in the literature.

Stochastic models for the propagation and rupture can be broken down into two families. The first one corresponds to purely statistical modeling of crack propagation data while the second is based on stochastic models derived from phenomenological laws and are random versions of the deterministic models presented above.

Statistical Modeling.

Empirical Models. A first kind of models consists in finding the statistical distribution which best represents the data and which takes into consideration their dispersion. For exemple in [43] authors used descriptive statistics to investigate

the distribution of the number of loading cycles needed by crack size to reach specific values or the distribution of crack sizes at specific loading cycles. Normal, lognormal and Weibull probability distribution functions were used to fit 51 different datasets. Authors conclude that the random loading cycles were best fitted by lognormal probability distribution (45/51) while random crack sizes were best fitted by Weibull probability distribution (29/51). This type of modeling seems adequate to describe a specific dataset but not flexible enough to be extended to several datasets or to prediction. Moreover, in this same paper, authors have shown that models that take into account the phenomenological laws (Paris' law (2.2) for example) and the temporal aspect are better adapted to describe the randomness of fatigue.

Jumps Models. These models were introduced by Bogdanoff and Kozin in [6] and they have since been used by other authors as Kirkner et al. [23]. In both cases, authors try to model the process of crack length a_t in continuous time, by a cumulative jump random process that is a MC in continuous time (Markovian jump process). In this case, there is no hazard on transitions because the process evolves deterministically from a state to the next one. On the other hand there is randomness on the time spent in each state who follows an exponential distribution. When the crack size increases, it is possible to model the propagation acceleration by increasing the parameter of the exponential variable.

The McGill-Markov model, introduced by Bodganoff and Kozin in [6], is an inhomogeneous jump model. It directly models the temporal evolution of the crack size by a random process that is defined as follows.

- The crack length a_t at time t evolves as a MC, that means the next crack length evolution depends only on its current length, not on its history.
- The law of the process dynamics is given by the transition probability. Given two times $t < t'$, this probability is defined by

$$\mathbf{P}(a_{t'} = j | a_t = i) = p_{ij}(t, t') = C_{j-1}^{j-i} q(t, t')^i (1 - q(t, t'))^{j-1},$$

with

$$q(t, t') = \exp(-\Delta(t, t')) \quad \text{and} \quad \Delta(t, t') = \int_t^{t'} \frac{\lambda(1 + \lambda s)}{1 + \lambda s^\kappa} ds,$$

where λ and κ are the model parameters.

In [41] authors have shown that these models fit fairly well the data. Nevertheless, they have no physical interpretations but can be generalized in order to give them a meaning using Piecewise-Deterministic Markov Processes (PDMPs).

Stochastic Models Derived from Deterministic Laws.

Deterministic Laws with Random Variables. Some authors as Virkler et al. [39] or Tanaka et al. [37] have proposed the first random models of fatigue based on the phenomenological laws like the one of Paris. They have done this introducing randomness in the characteristic coefficients of the material (C and/or m in the case of Paris' law (2.2)), in order to account for the non-homogeneity of the material.

In a more recent paper [33], the authors also consider the parameters C and m of Paris' law (2.2) as random variables. From the analysis of experimental data they decide to model either C by a log-normal random variable or m by a normal random variable but they are not random together. It is therefore easy to estimate them and to calculate the reliability indicators of the model.

This approach goes well with a better description of the phenomenon. However, the authors do not seem to consider the possibility of having C and m random together while this is what the data tends to show. Moreover, this model ignores the possible changes of dynamics in the propagation of the cracks because the laws of C and m do not depend on time.

Deterministic Laws with Random Processes. The use of stochastic differential systems makes possible to describe the temporal variations of the dispersion profile. Stochastic models take the general form of the experimental laws (2.1) by adding a multiplicative factor that is a random process.

- Lognormal Processes. Yang and Manning have introduced this model in [44, 45]. They added a multiplicative random factor X_t to the general equation of deterministic models (2.1).

$$\frac{da_t}{dt} = X_t L(t, \Delta K_t, K_{\max}, K_c, \sigma_{\max}, a_t, R) = X_t Q(a_t)^b,$$

in which Q and b are constants. The multiplicative coefficient X_t depends on time, so it is a stochastic process. According to these authors, if the above random factor X_t is modeled as a stationary lognormal random process with a median value of 1 and a standard deviation σ_X, its auto-covariance function has the following form

$$\mathbf{C}\mathrm{ov}[X_t, X'_t] = \sigma_X^2 \exp(-\zeta|t' - t|).$$

and the probability structure of the stochastic fatigue crack growth process can be obtained analytically. The success of this model is the fact that there are only two parameters to estimate: the standard deviation parameter σ_X and the covariance parameter ζ. If ζ tends to 0, we find the model with random variables because, for all t, $X_t = X_0$ and there is no longer dependence in time.

Wu and Ni in [41, 42, 43] have tested this model on experimental data and concluded that the simplest lognormal model is sufficient to describe the studied fatigue crack growth data. However, the hypothesis of process stationarity can be questioned because the rate of evolution of the cracks follows different phases over time, with in particular an acceleration phase just before the rupture. Moreover, in order to perform the reliability calculations it is necessary to know the law of

$$W_T = \int_0^T X_t dt.$$

Without any mathematical justification, the authors assume that the process (W_t) still follows a lognormal law whose parameters can be linked to those of the process X. There is no ongoing discussion on the validity of this approximation.

In [32] the authors modeled the expectation of the crack length $\mu_t = \mathbf{E}[a_t]$ by a deterministic law that looks like Paris's law,

$$\frac{d\mu_t}{dt} = C(\Delta K_t)^m. \tag{2.6}$$

Using Karhunen-Loève expansion, they proposed a stochastic model in which they consider that the crack length has the lognormal distribution instead of the more common assumption that growth rate is log-normally

distributed. The proposed model has been verified on the following experimental fatigue crack growth data [39] and [19] at different levels of constant amplitude. But these data contain only information on crack propagation and fracture regimes.

- Polynomial Law. Ni in [26] was inspired from the Yang model and proposed a polynomial stochastic fatigue crack growth model. This model is based on the assumption that the fatigue crack growth rate is equal to a deterministic polynomial function in terms of fatigue crack size. To take into account the statistical scatter of the fatigue crack growth, this function is multiplied by a stationary lognormal random factor,

$$\frac{da_t}{dt} = X_t(p + qa_t + ra_t^2). \tag{2.7}$$

In [27] the author verified results between analytical outcomes obtained from its proposed model and experimental data. These results appear satisfactory.

- Diffusion Processes (DPs). DP associated with SDE driven by a Brownian motion have been studied extensively in the literature for the modeling of crack propagation. The first attempt to model crack propagation by DPs was done by Sobczyk in [34]. They proposed an asymptotic approximation of the process a_t by diffusion that becomes valid when the parameter ϵ appearing in the propagation law tends to zero,

$$\frac{da_t}{dt} = \epsilon\, \widetilde{L}(a_t)X_t,$$

where $\widetilde{L}$ depends on ΔK_t, $K_{\max}$, K_c, $\sigma_{\max}$ and R that are known constants or functions of a_t. So $\widetilde{L}$ is only a function of the time and the crack length.

Asymptotic results and averaging techniques were initially developped by Stratonovich. They were then consolidated by other authors like Khas'minskii [21, 22] or Papanicolaou and Kholer [30], who allow to specify the conditions of approximation for a_t by a DP when ϵ tends to 0. Sobczyk in [34], based on these findings, was the first to try to model a_t by a DP. He showed that in the homogeneous case, the DP a_t is governed by a system of the form

$$da_t = \mu(a_t)dt + \sigma(a_t)dB_t,$$

where μ and σ are the drift and diffusion functions and B_t a brownian motion.

Lin and Yang in [25, 46] have completed these results by applying them to real cases. Since, the use of these processes has been declined by many other authors like Ivanova et Naess in [20] which use methods of numerical approximation of diffusion models for structural reliability calculations. These models have good mathematical justifications and allow to calculate indicators of reliability. The disadvantage of this type of model is related to the dynamics of the process a_t which fluctuates continuously over time, whereas growth is an intrinsic character of crack propagation.

3. PDMP Models for Propagation

In this section, we discuss the interest to use PDMPs for modeling crack propagation and present some models of the literature.

3.1. **Relevance of PDMP Models.** PDMPs are frequently used to model physical processes involved in the dynamics of industrial systems. Each physical process evolves according to a deterministic physical law until the occurrence of events of two types:

(1) the first type is directly linked to a deterministic evolution of the physical parameters of the process;
(2) the second type of event is purely stochastic.

It usually corresponds to random exogenous event or failures of system components. In this way, between two events, evolution of the system is based on physical laws and these ones take into account the dependencies or dynamical interactions between the different processes involved. Whatever the modeled phenomenon, it is of strong interest both to use deterministic laws – that come from physics or are well known by the practitioners – and to allow random events that come from the system itself (failure) or from outside.

Another interest of using PDMPs for modeling is that mathematical properties and numerical implementations for such processes have been extensively developed [10, 11]. For instance, in [13, 7], de Saporta et al. propose numerical methodology to perform optimal stopping on PDMPs or hidden PDMPs. [12] gives numerical method for impulse control of PDMPs. These sophisticated tools allow the computation of quantities of interest like the expected value of the remaining life (before failure or rupture), the probability to reach a threshold or to fail before a given time. Such tools allow the design of maintenance policy that takes into account the history of the system. These methodology was used in [14, 3] in a context of reliability and system safety.

In the case of FCP, there is no physical law for the propagation, but, on the one hand, the crack length is clearly increasing with time and it does not allow the use of diffusive processes for modeling since they are not monotonous. On the other hand, the phenomenological law of Paris, or other laws like Forman or Walkers, work well in the regimes II and III and are well known by the mechanical engineers. Use of PDMPs to model FCP makes it possible to:

(1) use the deterministic laws of propagation like the one of Paris,
(2) introduce randomness accounting for the variability between different specimens (like between the cracks in the same experimental conditions),
(3) introduce randomness during the crack propagation,
(4) take into account more predictable event like the change between regime II and regime III.

We will see below that according to the objectives of the modeling, the second and the third points are not necessarily used together. About the second item, note that even if PDMPs are not DPs, the randomness given by the law of the jump endow these kind of processes with a great flexibility and versatility to model phenomena. Figure 3.4 shows simulations of PDMPs from a very simple model with only one jump and the same ODEs with two different sets of parameters before and after the jump. Dispersion and scattering of the bundle is due to only one jump per trajectory, and some of them are visible. For a theoretical study about points accessible by a PDMP, [5] gives some results on the long time behavior of a certain class of PDMPs related to a certain set of accessible points.

One of the great interest of modeling with PDMPs is that it is possible to model regime switching at time of jump. The stochasticity of the change is linked to

the randomness of the phenomenon in different ways. The change can occur at a predictable time when some components of the state process reach a threshold, then deterministically trigger a change of mode in the system (see for instance [47] for description and modeling of the heated tank. The change can also occur at a random epoch because of exogenous events, like an impact independent of the system dynamics. A third kind of jump can occur, in a stochastic way depending on the state of the process, typically through the jump rate $\lambda(\Phi(x,t))$; which seems interesting to model the transition time between propagation regimes II and III. Framework of PDMPs allow the jump time to depend on the state of the process, that is the length of propagation in our case: the longer the crack, the more likely the change is from linear regime II to regime III. In [2], authors propose a method to infer the jump rate in such a case.

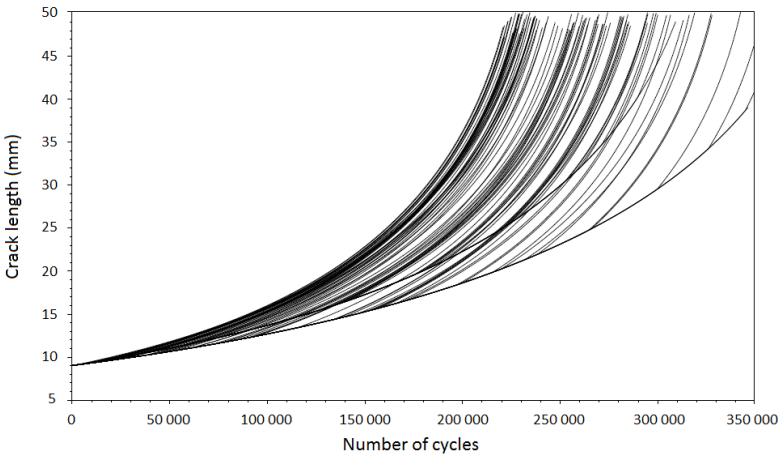

FIGURE 3.4. Simulation of crack propagation curves with only one jump and two modes before and after the jump.

3.2. **Multiplicative Model.** Chiquet, Limnios and Eid in [9] were the first to propose a PDMP for modeling crack propagation. This modeling allows to obtain a model based on well-known deterministic laws, to make the parameters of this law random and to allow regime changes in propagation. In this approach, the authors consider that fatigue crack growth changes through small shocks occurring at random times. They choose to use PDMPs without any constraint on the number of possible jumps associated with deterministic Paris' law and proposed a model derived from Paris' law, considering that the dimensionless factor $Y(a_t)$ appearing in (2.2) is approximately equal to one. They randomize the law with a multiplicative factor given by a jump Markov process P_t leading to the following stochastic dynamical system,

$$\frac{\mathrm{d}a_t}{\mathrm{d}t} = C(\Delta\sigma\sqrt{\pi})^m (a_t)^{m/2} P_t, \qquad a_0 = a. \tag{3.1}$$

The Markov process P_t is supposed to have a finite state space $\mathcal{P}$ and a constant matrix generator $Q = (q_{ij})_{(i,j)\in\mathcal{P}^2}$. Clearly, $(X_t)_{t\geq 0} = (a_t, P_t)_{t\geq 0}$ is a PDMP with

state space $\mathcal{X} = \mathbf{R}_+ \times \mathcal{P}$, jump rate given by $\lambda(x) = \lambda((a,p)) = \lambda(p) = q_{p,p}$ and jump kernel $Q(x,dy) = Q(p,p') = -q_{p,p'}/q_{p,p}$ given by the generator Q of Markov process. Parameters C and m are the same for the whole set of cracks so that each crack has its own process P_t. We can say that this term captures both randomness between cracks and during the propagation modifying crack growth rate da/dt. In [8], Chiquet fitted Virkler's data of propagation and highlights the acceleration of the jumps of the P_t's at the end of the propagations toward larger values announcing the instable regime III.

3.3. **One Jump Models.** In [38, 1, 4], in collaboration with mechanical engineers from Bordeaux University and EADS Astrium company, we have proposed two different models of crack propagation using PDMPs. We assumed that crack propagation can be expressed by a simple PDMP with only one change of regime. This allows to give a physical meaning to this jump and also to bring some flexibility to the model called regime-switching model. The objectives of the modeling were different for the two models.

For the first one, the objective was to capture and analyze the time transition between the linear regime II and instable regime III. For this, a regime switching model was really appropriate and we proposed the following simple model. At first, crack length evolves according to Paris' law given by (2.2) with parameters C and m chosen at random. After a random time, the model switches from Paris' law to Forman's law given by (2.4) with new parameters C and m. There is only one change in the propagation. In this case, $X_t = (a_t, P_t)$, a_t is the length of the crack; P_t is a mode with three components $P_t = (L_t, C_t, m_t)$ where $L_t \in \{1,2\}$ indicates the law of propagation and (C_t, m_t) are parameters of this law, which are constant before and after the jump. The initial value of L_t is deterministically equal to 1 and the transition is also deterministic from 1 to 2. $L_0 = 1$ and $Q((1,C_1,M_1),(2,.,.)) = 1$.

For the second model, the objective was to design a method of prediction of a given crack according to the first points of observation. This method of prediction is based on a model of PDMPs simpler than the previous one. Again we consider only one jump, but the deterministic flow is given by Paris' law before and after the jump. When a jump occurs, parameters of Paris' law change in a stochastic manner but the flow does not switch toward Forman's law. Indeed, the modeling of the crack propagation with two successive ODEs given by Paris' law fits well the data, the jump gives versatility and flexibility for the fitting and the "second" Paris' law is natural because the method of prediction is designed to predict crack propagation with information about the start of it, at the beginning of the Paris regime. In this case, $X_t = (a_t, P_t)$, a_t is the length of the crack; P_t is a mode with two components $P_t = (C_t, m_t)$ where (C_t, m_t) are parameters of this law.

Whatever the modeling, to study the characteristics of the crack at the jump time between the regimes II and III (model 1) or to build a model of propagation useful for the prediction (model 2), the manner to use the Virkler's data was to replace each experimental curve by the best possible theoretical curve issued from the chosen model (that is with the two given laws of propagation and only one jump). A theoretical curve i is determined by the values of five parameters: that of the first part law of propagation that we denote from this moment forward (m_1^i, C_1^i), the time of transition T^i and the parameters of the second part (m_2^i, C_2^i). For each model, we obtained a set of 68 vectors of parameters $(m_1^i, C_1^i, T^i, m_2^i, C_2^i)_{1 \le i \le 68}$.

The method to infer them is similar to a method of rupture detection, which is detailed in Subsection 4.1.

Now, let us give the results of this fitting of experimental curves by theoretical ones. For both models, the whole crack propagation is well fitted. Figure 3.5 displays graphs of the worst (left) and the best (right) fitted versions of the experimental curves among the 68's. If we consider distance between experimental and theoretical cracks on the whole trajectory, the model with Paris' law before and after the jump is the best one. But the regime switching model using Forman's law after the transition is better to account for the change at the end of the propagation. As shown in Figure 3.6, the end of crack propagation is accurately described, and the change between regimes II and III is captured by the regime switching of the PDMP.

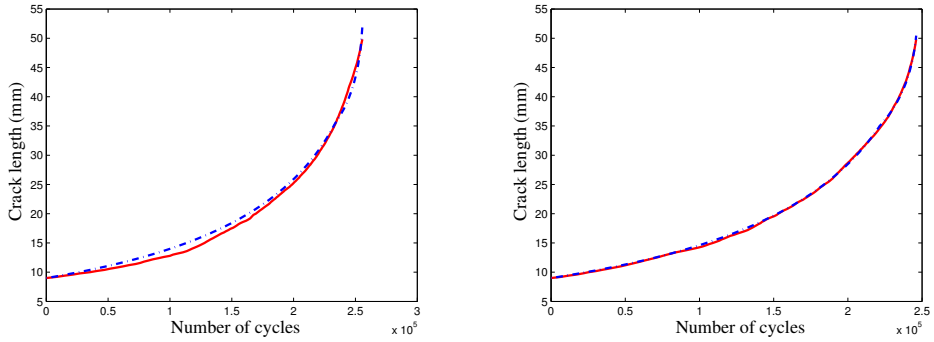

FIGURE 3.5. Experimental (solid line) and theoretical (dashed line) curves for the worse fitted propagation length curve (left) and for the best one (right).

Concerning the results of the model from Paris to Forman, it was interesting to analyze the time of transition and the characteristics of the crack at this time : they are given in Table 3.2. As expected, change of regime occurs at the end of the propagation. From a mechanical point of view, the study of the range value of the stress intensity factor ΔK_t at the time of transition gives information on the fracture toughness K_C, which is a quantity whose estimation is difficult and requires heavy experimentations. The results are analyzed in [4].

	Mean	Standard dev.	Min	Max
Crack length (mm)	39.53	4.55	30.40	48.20
Transition times (number of cycles)	241401	19184	192389	296091
ΔK_t (MPa$\sqrt{m}$)	20.8	1.0544	16.5	25.3
K_C (MPa$\sqrt{m}$)	25.8	NA	20.6	32

TABLE 3.2. Statistics concerning the crack length at transition, the transition times in terms of number of cycles and the corresponding stress intensity factor range.

About the result of prediction, we used the model from Paris to Paris to propose a method of prediction of a crack according to the first points of measure.

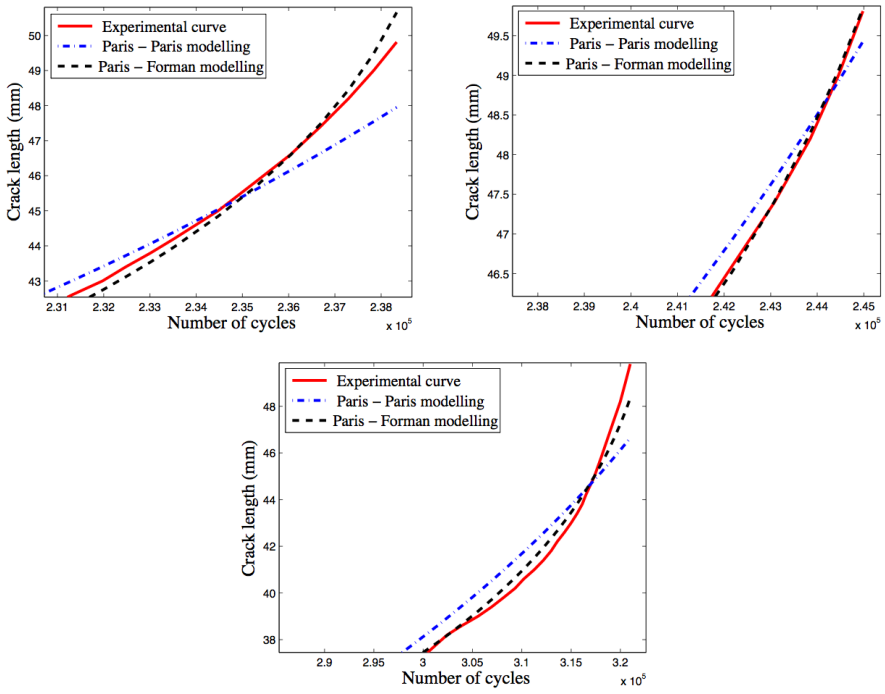

FIGURE 3.6. End of propagation for three different experimental cracks and fitting by regime-switching models with Paris' and Forman's law for the second regime.

We start with the model elaborated from the theoretical curves inferred with the rupture detection method described in Subsection 4.1. The model is described by the following elements:

(1) the flow of propagation given by Paris' law (2.2) before and after the jump,
(2) the state space $\mathcal{P}$ for the parameters (m, C),
(3) the initial distribution of (m_1, C_1), given by a probability distribution on $\mathcal{P}$,
(4) the law of the jump time depending on the parameters (m_1, C_1),
(5) the law of transition between the parameters of the first regime (m_1, C_1) and that of the second one (m_2, C_2).

We used this model with four possible values for (m_1, C_1), two others for (m_2, C_2) and constant jump rates $\lambda(m_1, C_1)$ to simulate the bundle of cracks of Figure 3.4 plausible to model together the 68 experimental cracks of Virkler's data.

It is clear that experimental cracks do not grow in the same way: some of them have high growth rate from the beginning to the end, while others are slower. The idea of the updating method is to use the information of the first points of the propagation of a given experimental crack in order to reduce the number of possible trajectories of the model: it means that the set of parameters $(m^{(j)}, C^{(j)})$ in $\mathcal{P}$ is reduced to predict the future of the propagation. It leads to a restricted and precise bundle of crack paths. Suppose that we have ℓ measures from an

experimental curve. Paris' model contains p theoretical curves corresponding to p values of $(m^{(j)}, C^{(j)})$ for the first part of the propagation. For a given experimental curve h, with ℓ points of measure, it is easy to compute a distance with each of the p theoretical curves of the model for the beginning of the propagation by

$$f(m, C) = \sum_{i=1}^{\ell} (a^i_{\text{th}}(m, C) - a^i_{\text{exp}})^2, \tag{3.2}$$

where $a^{j,k}_{\text{th}}$ and $a^{j,k}_{\text{exp}}$ are respectively the theoretical and experimental crack lengths at measurement k.

For each of the 68 experimental curves, we proceed in two steps:

(1) We compute the p values $f(m^{(j)}, C^{(j)})$ in order to choose the r $(r < p)$ nearest curves among the p theoretical curves of the modeling. The top of Figure 3.7 summarizes this procedure for $p = 10$ and $r = 4$: the experimental measures are drawn with crosses and we choose here the 4 nearest theoretical curves (dashed lines) among the $p = 10$ possible paths in the modeling.

(2) Now we work with each of the r possible trajectories chosen at the first step corresponding to r values of $(m^{(j)}, C^{(j)})$. For a given crack and each number of cycle N_i corresponding to the point of measure a^i_{exp}, we draw the p possible paths starting from the point $(N_i, a^i_{\text{th}}(m, C))$ and compute the distance between the second part of the experimental curve. Again we choose the r nearest among the p possible. This step is illustrated at the bottom of Figure 3.7 for the jump time at the third measure with $p = 10$ and $r = 4$.

Now, it remains to simulate the prediction bundle of each crack with the r selected $(m^{(j)}, C^{(j)})$ for the first part of propagation. The jump time is $T_j \wedge t_{\ell-1}$ with T_j an exponential time with parameter λ_j of the Paris model and a transition matrix derived by truncation of the initial transition matrix to the $2r$ remaining modes. In Figure 3.8, we draw the two extremal curves of this bundle for three experimental cracks.

In order to tackle the versatility of the actualisation procedure, we propose a cross validation method based on principle of "Leave one out". The principle is the following: for each of the experimental cracks, we compute the parameters of the Paris model with the 67 remaining cracks. With the ℓ first points of propagation of the crack of interest, the obtained modeling is used to propose a prediction bundle. The method gives a set of prediction for each of the 68 curves and we study the quality of the prediction with the following criterion. We compute a distance between the crack and its prediction bundle, which is null if the crack remains inside the bundle along the propagation. This distance is precisely defined in [4] but Figure 3.8 gives an idea of the quality of the predictions for a given distance.

We summarized the results in Table 3.3. For this, we distinguish three different crack behaviors according to their speed, measured by the number of cycles (denoted N_{160}) reached at the end of propagation, i.e after 160 length measurements. Cracks are considered rapid for $N_{160} < 240\,000$ cycles, while they are slow for $N_{160} > 280\,000$ cycles. Figure 3.8 presents three experimental curves with their predicted bundle for two rapid cracks (top) and for a slow one (bottom). The normalized

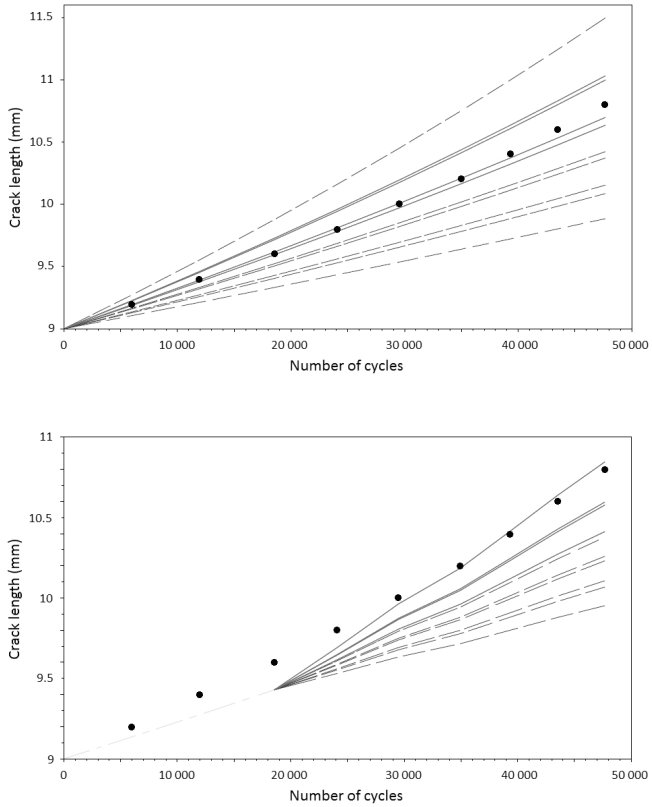

FIGURE 3.7. Top: first step of actualization method. Bottom: second step. Experimental measurements are drawn with crosses and continuous lines indicate the 4 nearest theoretical curves.

distance values D are calculated. For the quicker crack, the experimental curve stays inside its prediction bundle. The other rapid crack goes out of the bundle during a short time – around 125 000 cycles – and consequently the distance D is about 0.2. For the slow crack, the experimental curve does not predict well and the corresponding value of D is about 11.6. For all cracks, results of the cross validation are presented in Table 3.3. The parameter d_{160} indicates if the crack is in the bundle at the end of its propagation. Furthermore, we note that all the rapid cracks are well predicted ($0 < D^h < 1$) while any slow crack is accurately simulated ($D > 1$). For slow cracks and some mean cracks, when the crack path is not well simulated, the bundle is always situated above the experimental curve. This means that in this situation, the modeling always overestimates the real crack behavior and that the prediction will systematically reduce the risk of rupture. On the contrary, the prediction carried out for the quickest cracks and for a large number of mean cracks, which are the most dangerous in practice, is very powerful.

In this section, we introduced two models of crack propagation with PDMPs. With the first one, mechanical engineers were able to deduce information about

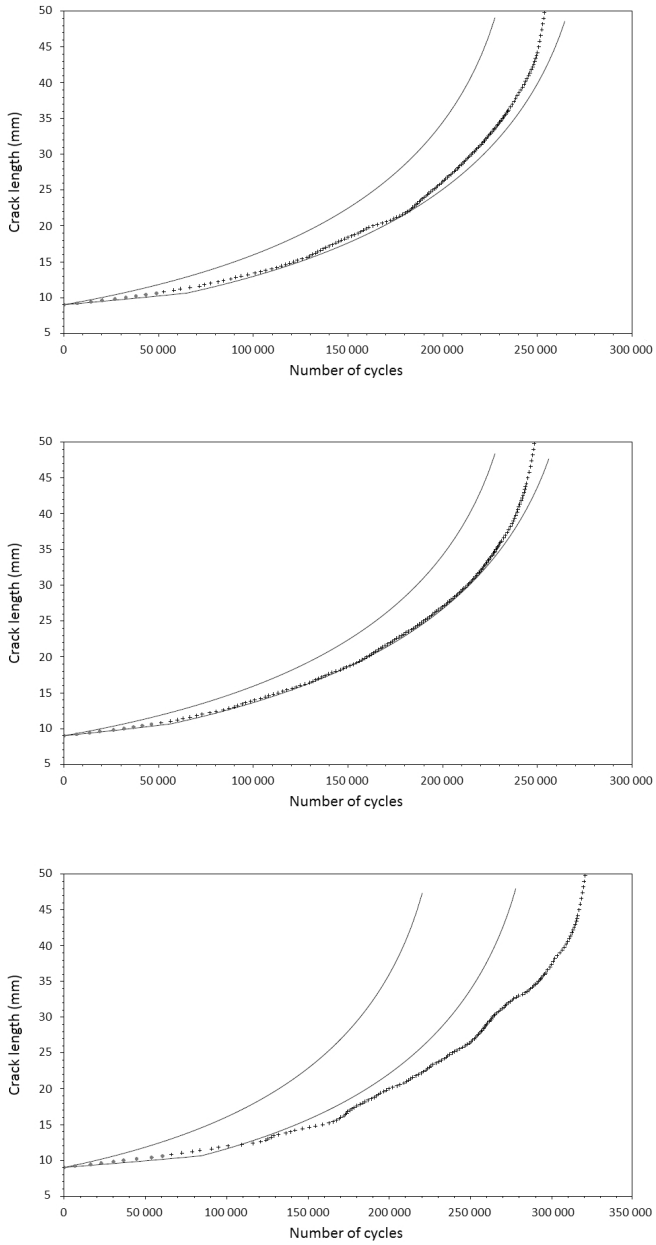

FIGURE 3.8. Three experimental curves with the extreme curves of the prediction bundle. From top to bottom, rapid crack with $D = 0$ and $D = 0.2$ and slow crack with $D = 11.6$.

	Quick crack	Mean crack	Slow crack
$D^h = 0$	8/11	18/50	0/7
$0 < D^h < 1$	11/11	38/50	0/7
$D^h > 1$	0/11	12/50	7/7
$d^h_{160} = 0$	9/11	35/50	1/7

TABLE 3.3. Normalized distance D and crack position at the end of the propagation d_{160} as a function of the type of crack.

the stress intensity factor at the transition of the linear regime II and the instable regime III. The second one is a first step of a prediction tool of experimental curve according to the first information about its propagation. We can claim that PDMP models, even if they are very simple, are relevant, and can be interpreted and give useful information on the mechanical processes involved in propagation.

4. Rupture Detection

In this section, we present two different ways to fit Virkler's data with PDMPs. Formally, if the proposed models do not allow the crack length to have discontinuities, fitting consists in detecting the changes of regime for the PDMP, i.e. to detect rupture in its dynamics. The first point of view is the one of Subsection 3.3. Our model is very simple, we suppose that we have only one change of dynamics, that is only one rupture to detect. To detect this change in an experimental curve, we search for the theoretical curve of the model that is the nearest, see Subsection 4.1. The second possibility is to consider each curve of propagation as a hidden PDMP where, at each point of the measure, the deterministic flow leading to da_t/dt is noised by a Gaussian variable. Algorithm and results on Virkler's data are given in Subsection 4.2. Whatever the viewpoint, it is necessary to determine epochs of transition for the fitting of the data and the construction of the model. Formally, it consists in detecting the change of regime for the PDMP. The next subsection is devoted to the presentation of the methods used in our different works, for this purpose.

4.1. Length a_t vs time t.

This section is devoted to the determination, for each experimental curve, of the nearest theoretical curve coming from the first model of Subsection 3.3. We tackle this problem with an optimisation problem formulation. By definition of our model, a theoretical curve is determined by five parameters $Z = (m_1, C_1, T, m_2, C_2)$ with (m_1, C_1) the Paris' law parameters and (m_2, C_2), the Forman's law parameters and T the jump time. Thus, to properly fit each of the 68 experimental curves with a theoretical one, we must determine the optimal parameters denoted by $Z^* = (m_1^*, C_1^*, T^*, m_2^*, C_2^*)$ that minimise an objective function. The latter measures the distance between crack lengths given by the experimental curve and a theoretical one obtained by discretisation of deterministic laws. The optimisation problem can be stated as follows for each curve $j \leq 68$,

$$Z^* = \underset{Z \in \mathbf{R}_+^5}{\arg\min}\, f^j(Z) = \sum_{k=1}^{164} \left[a_{\text{th}}^{j,k}(Z) - a_{\text{exp}}^{j,k} \right]^2. \tag{4.1}$$

Each point k of measure of a curve j is associated with the number of cycles N_k^j needed by curve j to reach length of the crack $a_{\text{exp}}^{j,k}$. The number of cycles plays

the role of time t in (2.2) and (2.4). Note that according to the typical design of measures described in Subsection 1.1, $a_{\text{exp}}^{j,k}$ does not depend of j but only N_k^j does. The theoretical length $a_{\text{th}}^{j,k}(Z)$ is computed by a Runge-Kutta scheme of order 4 for the solution of the ODE (2.2) with parameter (m_1, C_1) at time $t = N_k^j$ if $N_k^j \leq T$; if not, we compute it until time T and then solve ODE (2.4) starting from $a_{\text{th}}(Z, T)$ at time 0 and until $N_k^j - T$.

We have chosen to perform a simulated annealing algorithm to solve the above optimisation problem in (m_1, C_1, m_2, C_2) for a grid of times T. The initial value assigned to Z was randomly selected from a range of value. The use of a metaheuristic algorithm is justified by its ability to determine the global optimum for highly non-linear constrained optimisation problems. The reader can find further information about the implementation of simulated annealing algorithms and parameter selection in [16, 15].

4.2. **Growth Rate da_t/dt vs ΔK_t in Log Scale.** In this section, we present another way to model one curve of crack propagation. Unlike the previous Subsection 3.3, here we are interested in the typical logarithmic curve of the crack growth rate da_t/dt versus the stress intensity factor ΔK_t as shown in Figure 1.1 of Section 1. For that purpose, second order polynomial regression models seem to be appropriate to model this curve. We would like to estimate the polynomial regression models parameters and the time of transition between the linear regime II and the unstable regime III.

The studied model, as shown in Figure 4.9, is simple. It consists in two regimes separated by a time of transition T. Each of them is a second order polynomial regression model. Let us give some notations:

- the measurement times $X_1, \cdots, X_n$ are fixed;
- the regime variable is denoted by Z_i, $Z_i \in \{1, 2\}$. The two regimes are consecutive;
- the time of transition between the two regimes is denoted by T;
- the speed of propagation at X_i is denoted Y_i. When $Z_i = z$, Y_i is given by the following equation,

$$Y_i = a_z X_i^2 + b_z X_i + c_z + \epsilon_{i,z}, \qquad \text{for } z \in \{1, 2\} \text{ and } 1 \leq i \leq n, \tag{4.2}$$

where $\epsilon_{i,z} \sim \mathcal{N}(0, \sigma_z^2)$. Note that the change concerns not only parameters of the polynomial but also the variance of the noise.

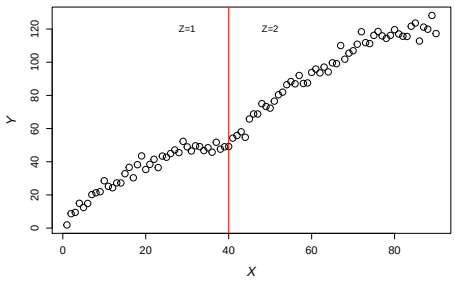

FIGURE 4.9. Example of one curve of the simulated model.

The regime variable Z_i is deterministic and takes its values according to X_i and T by the relation

$$Z_i = \begin{cases} 1 & \text{if } X_i < T, \\ 2 & \text{else.} \end{cases} \tag{4.3}$$

This relation can be rewritten as $\mathbf{P}(Z_i = 1|X_i) = \mathbb{1}_{\{X_i<T\}}$.

Our objective is to estimate the polynomial parameters of the two regimes: a_1, b_1, c_1, σ_1^2, a_2, b_2, c_2, σ_2^2 and time of transition T, parameters that are denoted by the vector θ,

$$\theta = \left(a_1, a_2, b_1, b_2, c_1, c_2, \sigma_1^2, \sigma_2^2, T\right)^t.$$

Let us now define some useful conditional probability functions:

- $\mathbf{P}_\theta(Z|X)$ is the conditional probability function of Z given X defined by (4.3).
- $h_\theta(Y, Z|X)$ is the conditional probability function of Y and Z given X defined by
$$h_\theta(Y, Z|X) = \omega_\theta(Y|Z, X)\mathbf{P}_\theta(Z|X),$$
where
- $\omega_\theta(Y|Z, X)$ is the conditional probability density function of Y given Z and X,
$$\omega_\theta(Y|Z, X) = \frac{1}{\sqrt{\sigma_Z^2 2\pi}} \exp\left(\frac{-(Y - (a_Z X^2 + b_Z X + c_Z))^2}{2\sigma_Z^2}\right),$$
where a_Z, b_Z, c_Z and σ_Z^2 depend on the regime variable Z.
- $g_\theta(Z|Y, X)$ is the posterior probability distribution of Z given X and Y given by
$$g_\theta(Z|Y, X) = \frac{h_\theta(Y, Z|X)}{f_\theta(Y|X)} = \frac{\omega_\theta(Y|Z, X)\mathbf{P}_\theta(Z|X)}{\sum_{k=1}^{2} \omega_\theta(Y|Z, X)\mathbf{P}_\theta(Z|X)}.$$

With these notations, we can write the complete log-likelihood of the model

$$L((Y_i, Z_i)_{1\le i\le n}, \theta|(X)_{1\le i\le n}) = \sum_{i=1}^{n} \log\left(\omega_\theta(Y_i|Z_i, X_i)\mathbf{P}_\theta(Z_i|X_i)\right). \tag{4.4}$$

Because T is not observed, the indicator functions coming from the $\mathbf{P}_\theta(Z_i|X_i)$ give an extreme rigidity to the model used for the inference of θ. It is why we modify the model to approach the likelihood by smoothing the indicators. To do so, we put some flexibility about the probability to be in a regime near the time of transition. Conditionally to the value of T the regime Z will now not be completely observed. It can be considered as a latent variable and its distribution $\mathbf{P}_\theta(Z|X)$, shown in Figure 4.10, is given by

$$\mathbf{P}_\theta(Z{=}1|X{=}x) = \mathbb{1}_{[0,T-e_1]} + \left(1 - \left[\frac{x - (T - e_1)}{e_1 + e_2}\right]^2\right)\mathbb{1}_{(T-e_1,T+e_2]}. \tag{4.5}$$

The flexibility is provided by the probabilities on the interval $[T-e_1, T+e_2]$ around T that are not 0 or 1. Parameters e_1 and e_2 are chosen in the following way.

- $T - e_1$: value of X such as 95% of the observations before T are lower than $T - e_1$;

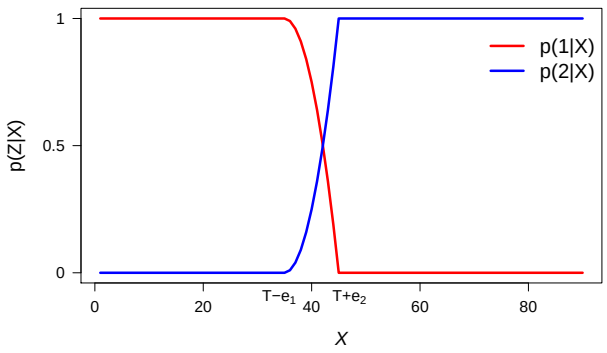

FIGURE 4.10. Probability of Z according to X.

- $T+e_2$: value of X such as 95% of the observations after T are greater than $T+e_2$.

In attendance of the latent variable Z, the classic method of maximum likelihood is not usable anymore. Indeed, all available variables need to be observed to calculate the complete log-likelihood. To estimate θ when all variables are not observable, the Expectation Maximization (EM) algorithm consists in replacing the complete log-likelihood by its conditional expected value given the observations. This algorithm is an iterative procedure for computing the maximum likelihood estimator when only a subset of the variables is observed. The l^{th} iteration of the algorithm breaks down in two steps:

- E-step: considering $\hat{\theta}_{l-1}$ we compute the conditional expected value given the observations $\mathcal{L}(Y;\theta,\hat{\theta}_{l-1})$ defined in (4.6);
- M-step: we find the parameters $\hat{\theta}_l$ that maximizes $\mathcal{L}(Y;\theta,\hat{\theta}_{l-1})$ in θ.

$\mathcal{L}(Y;\theta,\hat{\theta}_{l-1})$, the conditional log-likelihood at the l^{th} iteration of the EM algorithm is given by

$$\begin{aligned}\mathcal{L}(Y;\theta,\hat{\theta}_{l-1}) &= \mathbf{E}(\log(L(Y,Z,\theta|X))|X,Y)\\ &= \sum_{i=1}^{n}\int g_{\hat{\theta}_{l-1}}(z|Y_i,X_i)\log(h_\theta(Y_i,z|X_i))dz. \qquad (4.6)\end{aligned}$$

Note that with this definition, at step M, the conditional probability given (X,Y) for Z to be in a regime is considered as known and the optimization concerns the function h_θ. By integrating the conditional log-likelihood with respect to the counting measure on $\{1,2\}$ for Z, it can be rewritten as

$$\begin{aligned}\mathcal{L}(Y;\theta,\hat{\theta}_{l-1}) &= -\frac{n}{2}\log(2\pi)+\sum_{z=1}^{2}\sum_{i=1}^{n} g_{iz}\log(\mathbf{P}_\theta(z|X_i))\\ &\quad -\frac{1}{2}\sum_{i=1}^{n}\sum_{z=1}^{2}\Big[\log(\sigma_z^2)+\frac{(Y_i-(a_zX_i^2+b_zX_i+c_z))^2}{\sigma_z^2}\Big]g_{iz},\end{aligned}$$

where $g_{iz} = g_{\hat{\theta}_{l-1}}(z|Y_i, X_i)$.

The variable T is hidden in the probability $\mathbf{P}_\theta(z|X_i)$. That makes it difficult to optimize according to the whole components of the vector θ. For this reason we divide the problem into two parts. The first part corresponds to the research of T and the second part corresponds to the estimation of $\widetilde{\theta}$, which is given by

$$\widetilde{\theta} = \left(a_1, a_2, b_1, b_2, c_1, c_2, \sigma_1^2, \sigma_2^2\right)^t.$$

Let us consider the problem if T is known. We would like to estimate $\widetilde{\theta}$ by maximizing the conditional log-likelihood, given the observations. Because piecewise-polynomial regression models admit continuity between the two regimes, maximization needs to be done under a continuity constraint at times of transition, that is given by

$$q(\theta) = a_1T^2 + b_1T + c_1 - a_2T^2 - b_2T - c_2 = 0.$$

To do this optimization, we made the choice to use Lagrange multiplier method. This method is a strategy for finding the local maxima or minima of a function subject to constraints. It states that if there is an extremum in $\widetilde{\theta}$, then there exists μ, the Lagrange multiplier associated to constraints, such that

$$\nabla\mathcal{L}(Y; \theta, \hat{\theta}_{l-1}) = \mu\nabla q(\theta).$$

Parameter μ has to be evaluated so that we incorporate it in the parameters to estimate and split them into two parts $\breve{\theta} = (a_1, a_2, b_1, b_2, c_1, c_2, \mu)^t$ and $\sigma^2 = \left(\sigma_1^2, \sigma_2^2\right)^t$ such that the system to resolve can be written in the following way

$$\begin{cases} M(\sigma^2)\breve{\theta} = \gamma, \\ \sigma^2 = f(\breve{\theta}). \end{cases}$$

Let us define g_{i1} and g_{i2} such as $g_{i1} = g_{\hat{\theta}_{l-1}}(1|Y_i, X_i)$ and $g_{i2} = g_{\hat{\theta}_{l-1}}(2|Y_i, X_i)$. γ depends on the observed data (X_i, Y_i), σ^2 and $\hat{\theta}_{l-1}$. It is given by

$$\gamma = 0, \sum_{i=1}^{n} X_i^2Y_ig_{i1}, \sum_{i=1}^{n} X_i^2Y_ig_{i2}, \sum_{i=1}^{n} X_iY_ig_{i1}, \sum_{i=1}^{n} X_iY_ig_{i2}, \sum_{i=1}^{n} Y_ig_{i1}, \sum_{i=1}^{n} Y_ig_{i2}{}^t.$$

M is a 7×7 matrix that only depends on T, σ^2 and $\hat{\theta}_{l-1}$,

$$M = \begin{bmatrix} T^2 & -T^2 & T & -T & 1 & -1 & 0 \\ \sum_{i=1}^{n} X_i^4g_{i1} & 0 & \sum_{i=1}^{n} X_i^3g_{i1} & 0 & \sum_{i=1}^{n} X_i^2g_{i1} & 0 & -T^2\sigma_1^2 \\ 0 & \sum_{i=1}^{n} X_i^4g_{i2} & 0 & \sum_{i=1}^{n} X_i^3g_{i2} & 0 & \sum_{i=1}^{n} X_i^2g_{i2} & T^2\sigma_2^2 \\ \sum_{i=1}^{n} X_i^3g_{i1} & 0 & \sum_{i=1}^{n} X_i^2g_{i1} & 0 & \sum_{i=1}^{n} X_ig_{i1} & 0 & -T\sigma_1^2 \\ 0 & \sum_{i=1}^{n} X_i^3g_{i2} & 0 & \sum_{i=1}^{n} X_i^2g_{i2} & 0 & \sum_{i=1}^{n} X_ig_{i2} & T\sigma_2^2 \\ \sum_{i=1}^{n} X_i^2g_{i1} & 0 & \sum_{i=1}^{n} X_ig_{i1} & 0 & \sum_{i=1}^{n} g_{i1} & 0 & -\sigma_1^2 \\ 0 & \sum_{i=1}^{n} X_i^2g_{i2} & 0 & \sum_{i=1}^{n} X_ig_{i2} & 0 & \sum_{i=1}^{n} g_{i2} & \sigma_2^2 \end{bmatrix}.$$

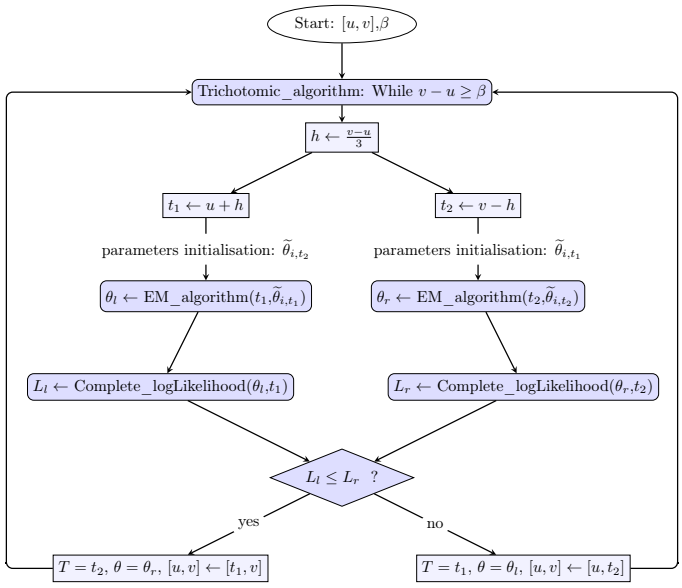

FIGURE 4.11. Outline of the global procedure.

$f(\breve{\theta})$ is a non linear function taking values in $\mathbf{R}^2$ defined by

$$f(\breve{\theta}) = \begin{pmatrix} \dfrac{\sum_{i=1}^{n} (Y_i - (a_1 X_i^2 + b_1 X_i + c_1))^2 g_{i1}}{\sum_{i=1}^{n} g_{i1}} \\ \dfrac{\sum_{i=1}^{n} (Y_i - (a_2 X_i^2 + b_2 X_i + c_2))^2 g_{i2}}{\sum_{i=1}^{n} g_{i2}} \end{pmatrix}.$$

This non linear part forces us to solve this system by using a fixed point method.

Let us now consider the estimation of time of transition T. For this, we use a trichotomic algorithm. This algorithm allows to calculate the maximum of a concave function ℓ defined on a known time interval $[u, v]$. It consists in dividing in three equal parts the time interval $[u, v]$. Let us define $h = \frac{v-u}{3}$, $t_1 = u + h$ and $t_2 = v - h$,

- if $\ell(t_1) \leq \ell(t_2)$ then the $[u, v]$ interval becomes $[t_1, v]$;
- if $\ell(t_1) \geq \ell(t_2)$ then the $[u, v]$ interval becomes $[u, t_2]$.

In our case,

- At the first step, the interval $[u, v]$ corresponds to the interval of the observations $[X_1, X_n]$;
- t_1 and t_2 are the times of transition that we compare;
- ℓ corresponds to the complete log-likelihood given by (4.4).

This algorithm stops when the difference between the two interval bounds is smaller than a fixed value β. To obtain our final algorithm, we combine the EM and trichotomic algorithms as presented in Figure 4.11.

As explained in Subsection 3.3, we used the Virkler's data by replacing each experimental curve by the best possible theoretical curve issued from the piecewise polynomial regression model. A theoretical curve i studied over the form da_t/dt vs ΔK_t in log scale is determined by the values of nine parameters: the parameters of the first regime $(a_1^i, b_1^i, c_1^i, \sigma_1^{2i})$, the time of transition T^i, and the parameters of the second regime $(a_2^i, b_2^i, c_2^i, \sigma_2^{2i})$.

If we consider distance between experimental and theoretical crack growth rate on the wole trajectory, Figure 4.12 (4.13, respectively) displays graphs of the worst and the best fitted versions of the experimental curves da_t/dt vs ΔK_t (a_t vs t, respectively) among the 68s. Even if Figure 4.12 shows difference between the experimental and the fitted growth rate, this difference is well smoothed when we draw the corresponding trajectories of a_t vs t in Figure 4.13. This one has to be compared with the fitting by switching ODEs of Figure 3.5. In each case, the model fits the crack growth evolution very well and we can note that in both model the worst fitting concerns the same crack. It is the slowest crack of the Virkler's data in both case (we can see oscillations in the growth rate as if some grains in the alloy have slowed down the propagation).

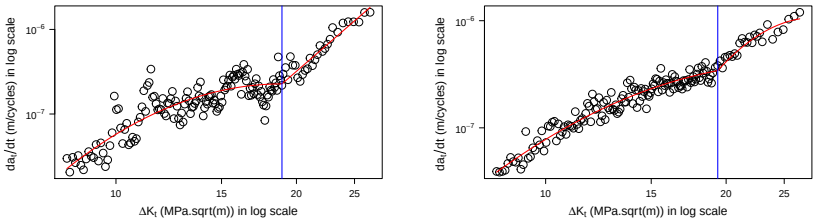

FIGURE 4.12. Experimental (points) and theoretical (line) curves for the worst fitted propagation curve (left) and for the best one (right) in the da_t/dt vs ΔK_t representation. Vertical lines show the time of transition between regimes II and III.

About the results of this model, it was interesting to analyze the time of transition and the characteristics of the crack at this time. They are given in Table 4.4. As observed with fitting switching ODEs, change of regimes occurs at the end of the propagation.

	Mean	Standard dev.	Min	Max
Crack length (mm)	43.1	3.27	36	49
Transition times (number of cycles)	248758	18957	209128	303893
ΔK_t (MPa$\sqrt{m}$)	22.47	1.74	18.9	25.9
K_C (MPa$\sqrt{m}$)	28.1	NA	23.64	32.46

TABLE 4.4. Statistics concerning the crack at transition, the transition times in terms of number of cycles and the correspond stress intensity factor range.

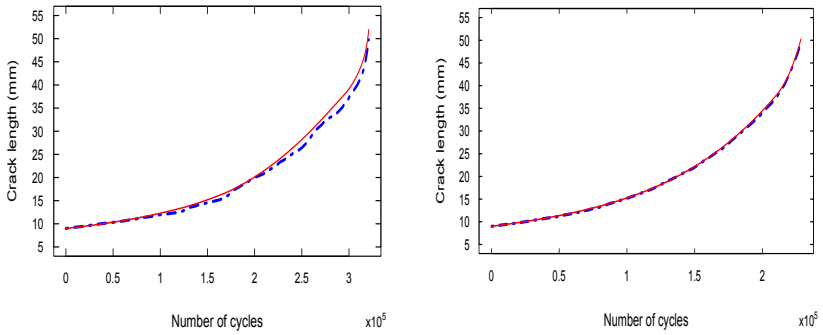

FIGURE 4.13. Experimental (solid line) and theoretical (dashed line) curves for the worst fitted propagation curve (left) and for the best one (right) in the a_t vs t.

The main part of the present work is the application of the EM algorithm in piecewise polynomial regression versus fitting switching ODEs to the data set of Virkler et al. [39]. These two models are used when the propagation has two regimes and one unique time of transition. They are different because they model different quantities issued from the data. Fitting switching ODE models crack propagation evolution (a_t versus t) whereas EM algorithm in piecewise polynomial regression models crack growth rate evolution (da_t/dt versus ΔK_t) which seems to be more scattered. Models and the number of parameters to estimate are different (seven for Paris and nine for the polynomial regression).

Regarding the rupture detection, the two optimization methods we propose are really different. The first one is using simulated annealing to estimate model parameters and T is optimized across a grid of time. For the second one, to estimate the model parameters a more statistical approach is set up, thanks to an EM algorithm, while the transition time T is estimated by a trichotomic algorithm. In both cases, the estimations of the model parameters and time of transition are separated.

Moreover, the estimation results of the transition times using the two methods are drawn in Figure 4.14, and we can see that they are well correlated and that polynomial models give greater values than switching ODE models. Because the real time of transitions are unknown, we cannot conclude what is a best model or method. However, if we consider the computation time needed for the estimation, there is a great advantage to use the EM algorithm in piecewise polynomial regression, which is faster than fitting switching ODEs.

5. Conclusion and Perspectives

In this chapter, we have presented the interest to model crack propagation with PDMPs and presented two different methods of rupture detection for the fitting of these models. We have shown that even if the PDMP models are very simple, they are versatile enough to report propagation phenomenon, to help for their understanding and to propose prediction bundles for individual cracks. Results of

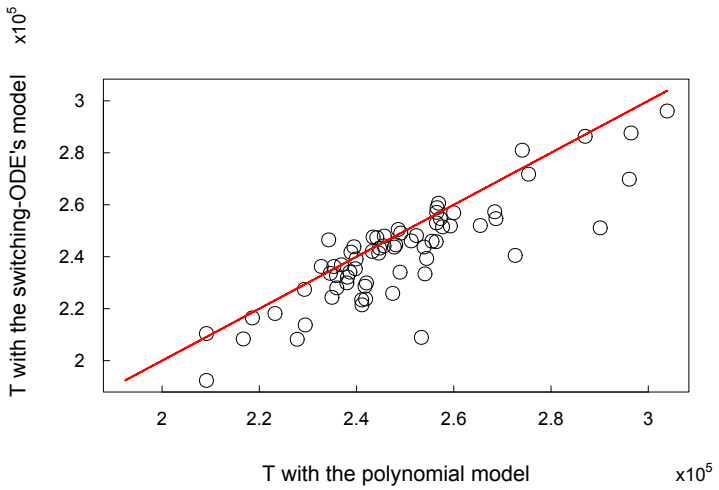

FIGURE 4.14. Comparison of the times of transition estimations obtained by EM algorithm in piecewise polynomial regression (abscissa) and fitting switching ODEs (ordinate).

these models make possible inference on the jump rate of the transition between regimes II and III according to the length of the crack as it has be done in [2] in a slight different switching ODE model (results shown in Figure 5.15).

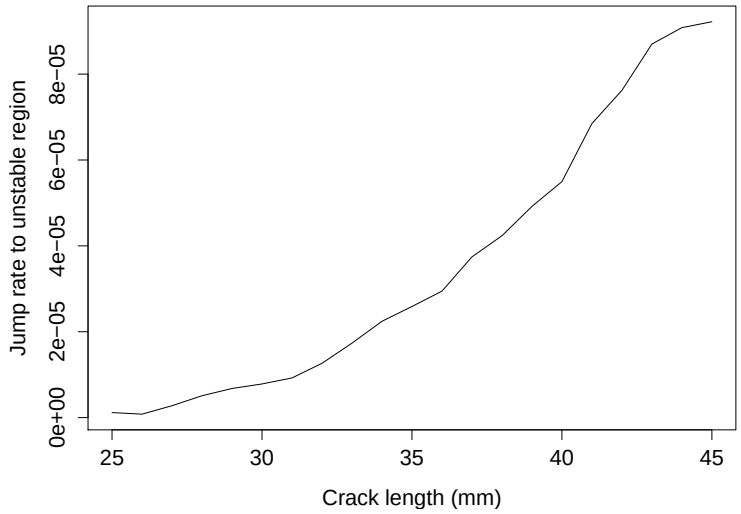

FIGURE 5.15. Estimated jump rate of a crack according to its length.

On the other hand, inference of PDMP models leads to the emergence of new questions for the statisticians who have to develop new methods. For instance, we

work now on an algorithm to detect jumps whose number is not determined. It is a very delicate problem to infer altogether number and times of jumps.

References

[1] R. Azaïs, C. Elegbede, A. Gégout-Petit, and M. Touzet. Estimation, simulation et prévision d'un modèle de propagation de fissures par des processus markoviens déterministes par morceaux. In *Actes du congrès lambd-mu 17 17e Congrès de Maîtrise des Risques et de Sûreté de Fonctionnement 5-7 octobre 2010 La Rochelle*, pages H5–C3, France, 2010.

[2] R. Azaïs and A. Muller-Gueudin. Optimal choice among a class of nonparametric estimators of the jump rate for piecewise-deterministic markov processes. *Electronic Journal of Statistics*, 10(2):3648–3692, 2016.

[3] C. Baysse, D. Bihannic, B. de Saporta, A. Gégout-Petit, M. Prenat, and J. Saracco. Maintenance optimisation of optronic equipment. In *Chemical Engineering Transactions*, Milano, Italy, September 2013. vol. 33, pp. 709–714.

[4] A. Ben Abdessalem, R. Azaïs, M. Touzet-Cortina, A. Gégout-Petit, and M. Puiggali. Stochastic modelling and prediction of fatigue crack propagation using piecewise-deterministic markov processes. *Journal of Risk and Reliability*, 230(4):405–416, 2016.

[5] M. Benaïm, S. Le Borgne, F. Malrieu, and P.A. Zitt. Qualitative properties of certain piecewise deterministic markov processes. *Annales de l'Institut Henri Poincaré (B) Probabilités et Statistiques*, 51(3):1040–1075, 2015.

[6] J.L. Bogdanoff and F. Kozin. *Probabilistic models of cumulative damage*. A Wiley-Interscience publication. John Wiley & Sons, Etats-Unis, 1985.

[7] A. Brandejsky, B. de Saporta, and F. Dufour. Optimal stopping for partially observed piecewise-deterministic markov processes. *Stochastic Processes and their Applications*, 123(8):3201–3238, 2013.

[8] J. Chiquet. *Modélisation et estimation des processus de dégradation avec application en fiabilité des structures*. PhD thesis, Université de Technologie de Compiègne, 2007.

[9] J. Chiquet, N. Limnios, and M. Eid. Piecewise deterministic markov processes applied to fatigue crack growth modelling. *Journal of Statistical Planning and Inference*, 139(5):1657 – 1667, 2009.

[10] M.H.A. Davis. Piecewise-deterministic markov-processes - a general-class of non-diffusion stochastic-models. *Journal Of The Royal Statistical Society. Series B-Methodological*, 46(3):353–388, 1984.

[11] M.H.A. Davis. *Markov models and optimization*, volume 49 of *Monographs on Statistics and Applied Probability*. Chapman & Hall, London, 1993.

[12] B. de Saporta and F. Dufour. Numerical method for impulse control of piecewise deterministic markov processes. *Automatica*, 48(5):779–793, 2012.

[13] B. De Saporta, F. Dufour, and K. Gonzalez. Numerical method for optimal stopping of piecewise deterministic markov processes. *Ann. Appl. Probab.*, 20:1607–1637, 2010.

[14] B. de Saporta, F. Dufour, H. Zhang, and C. Elegbede. Optimal stopping for the predictive maintenance of a structure subject to corrosion. *Journal of Risk and Reliability*, 226 (2):169–181, 2012.

[15] J. Dréo. *Metaheuristics for Hard Optimization: Methods and Case Studies*. Springer, 2006.

[16] V. Fabian. Simulated annealing simulated. *Computers & Mathematics with Applications*, 33(1–2):81 – 94, 1997.

[17] R. Forman, V. Kearney, and R. Engle. Numerical analysis of crack propagation in cyclic-loaded structures. *Journal of basic Engineering*, 89(3):459–463, 1967.

[18] R.G. Forman and S.R. Mettu. Behavior of surface and corner cracks subjected to tensile and bending loads in ti-6al-4v alloy. Technical report, National Aeronautics and Space Administration, 1990.

[19] H. Ghonem and S. Dore. Experimental study of the constant-probability crack growth curves under constant amplitude loading. *Engineering Fracture Mechanics*, 27(1):1–25, 1987.

[20] A. Ivanova and A. Naess. Importance sampling for dynamic systems by approximate calculation of the optimal control function. In *Proc. 4th Int. Conf. on Mathematical Methods in Reliability*, 2004.

[21] R.Z. Khas'minskii. A limit theorem for the solutions of differential equations with random right-hand sides. *Theory of Probability & Its Applications*, 11(3):390–406, 1966.

[22] R.Z. Khas'minskii. On stochastic processes defined by differential equations with a small parameter. *Theory of Probability & Its Applications*, 11(2):211–228, 1966.

[23] D.J. Kirkner, K. Sobczyk, and B.F. Spencer. On the relationship of the cumulative jump model for random fatigue to empirical data. *Probabilistic engineering mechanics*, 14(3):257–267, 1999.

[24] T. Kitamura, L.J. Ghosn, and R. Ohtani. Stochastic modeling of crack initiation and short-crack growth under creep and creep-fatigue conditions. Technical report, National Aeronautics and Space Administration, 1989.

[25] Y.K. Lin and Yang J.N. On statistical moments of fatigue crack propagation. *Engineering Fracture Mechanics*, 18(2):243–256, 1983.

[26] C.C. Ni. Formulation of a polynomial stochastic fatigue crack growth model. In *Advanced Materials Research*, volume 909, pages 467–471. Trans Tech Publ, 2014.

[27] C.C. Ni. Verification of a polynomial stochastic fatigue crack growth model. In *2015 International Conference on Intelligent Systems Research and Mechatronics Engineering*. Atlantis Press, 2015.

[28] R. Ohtani. Growth and distribution of microcracks at the surface of smooth specimen of 304 stainless steel in creep and effect of high temperature oxidation. *J. Soc. Mater. Sci., Jpn.*, 32(357):635–639, 1983.

[29] R. Ohtani, T. Kinami, and H. Sakamoto. Small crack propagation in high temperature creep-fatigue of 304 stainless steel. *Trans. Japan soc. Mech. Eng.(Ser. A).*, 52(480):1824–1830, 1986.

[30] G.C. Papanicolaou and W. Kohler. Asymptotic theory of mixing stochastic ordinary differential equations. *Communications on Pure and Applied Mathematics*, 27(5):641–668, 1974.

[31] P.C. Paris and F. Erdogan. A critical analysis of crack propagation laws. *Journal of Basic Engineering*, 85(4):528–533, 1963.

[32] A. Ray, S. Tangirala, and S. Phoha. Stochastic modeling of fatigue crack propagation. *Applied Mathematical Modelling*, 22(3):197–204, 1998.

[33] W. Shen, A.B.O. Soboyejo, and W.O. Soboyejo. Probabilistic modeling of fatigue crack growth in ti–6al–4v. *International journal of fatigue*, 23(10):917–925, 2001.

[34] K. Sobczyk. On the markovian models for fatigue accumulation. *Journal de Mécanique Théorique et Appliquée*, pages 147–160, 1982.

[35] K. Sobczyk and B.F. Spencer. Random microstructural effects on fatigue accumulation. *International journal of fatigue*, 17(8):521–530, 1995.

[36] R.I. Stephens, A. Fatemi, R.R. Stephens, and Fuchs H.O. *Metal fatigue in engineering*. A Wiley-Interscience publication. John Wiley & Sons, Etats-Unis, second edition, 2000.

[37] S. Tanaka, M. Ichikawa, and S. Akita. Variability of m and c in the fatigue crack propagation law. *International Journal of Fracture*, 17(5):R121–R124, 1981.

[38] M. Touzet, R. Azaïs, A. Gégout-Petit, C. Elegbede, and M. Puiggali. Modèle probabiliste de propagation de fissures de fatigue. In *20ème Congrès Français de Mécanique, 28 août/2 sept. 2011*, Besançon, France, 2011. AFM, Maison de la Mécanique, 39/41 rue Louis Blanc, 92400 Courbevoie, France (FR).

[39] D. Virkler, B. Hillberry, and P. Goel. The statistical nature of fatigue crack propagation. *J Engng Mater Technol*, 101(2):148 – 153, 1979.

[40] K. Walker. The effect of stress ratio during crack propagation and fatigue for 2024-t3 and 7075-t6 aluminum. In *Effects of environment and complex load history on fatigue life*. ASTM International, 1970.

[41] W.F. Wu and C.C. Ni. A study of stochastic fatigue crack growth modeling through experimental data. *Probabilistic Engineering Mechanics*, 18(2):107–118, 2003.

[42] W.F. Wu and C.C. Ni. Probabilistic models of fatigue crack propagation and their experimental verification. *Probabilistic Engineering Mechanics*, 19(3):247–257, 2004.

[43] W.F. Wu and C.C. Ni. Statistical aspects of some fatigue crack growth data. *Engineering Fracture Mechanics*, 74(18):2952–2963, 2007.

[44] J.N. Yang and S.D. Manning. Stochastic crack growth analysis methodologies for metallic structures. *Engineering Fracture Mechanics*, 37(5):1105–1124, 1990.

[45] J.N. Yang and S.D. Manning. A simple second order approximation for stochastic crack growth analysis. *Engineering Fracture Mechanics*, 53(5):677–686, 1996.

[46] J.N. Yangt. A stochastic theory of fatigue crack propagation. 1985.

[47] H. Zhang, F. Dufour, Y. Dutuit, and K. Gonzalez. Piecewise deterministic markov processes and dynamic reliability. *Proceedings of the Institution of Mechanical Engineers, Part O: Journal of Risk and Reliability*, 222(4):545–551, 2008.